SOIL Discuss., 2, 427–448, 2015
www.soil-discuss.net/2/427/2015/
doi:10.5194/soild-2-427-2015

Passive soil heating using an inexpensive infrared mirror design – a proof of concept

C. Rasmussen[1], **R. E. Gallery**[2,3], **and J. S. Fehmi**[2]

[1]Department of Soil, Water and Environmental Science, The University of Arizona, Tucson, AZ, USA
[2]School of Natural Resources and the Environment, The University of Arizona, Tucson, AZ, USA
[3]Department of Ecology and Evolutionary Biology, The University of Arizona, Tucson, AZ, USA

Received: 3 April 2015 – Accepted: 20 April 2015 – Published: 11 May 2015

Correspondence to: C. Rasmussen (crasmuss@cals.arizona.edu)

Published by Copernicus Publications on behalf of the European Geosciences Union.

Abstract

There is need to understand the response of soil systems to predicted climate warming for modeling soil process response to climate warming. Current methods for soil warming include expensive and difficult to implement active and passive techniques. Here we test a simple, inexpensive in situ passive soil heating approach, based on easy to construct infrared mirrors that do not require automation or enclosures. The infrared mirrors consisted of 61 × 61 cm glass panels coated with infrared reflecting film. The mirrors as constructed are effective for soil heating in environments typified by open canopy and low canopy vegetation. Mirror tests were performed on several soils in a warm semiarid environment. Results indicated that the infrared mirrors yielded significant heating and drying of soil surface and shallow subsurface relative to un-warmed control treatments, and that warming and drying effects was soil specific with greater potential warming on soils with lower volumetric heat capacity. Atmospheric and soil moisture attenuated mirror induced soil warming. The results demonstrate proof-of-concept that the infrared mirrors may be used to passively heat the near soil surface, providing an inexpensive, low-maintenance alternative to other passive and active soil heating technologies.

1 Introduction

Climate change and warming present significant challenges to understanding future ecosystem response, function, and management. The most recent projections suggest up to a 5 °C warming by the end of this century, with mean winter and summer warming of 3.8 °C and 3.3 °C, respectively (IPCC, 2014). Given these projections, there is pressing need to understand the response of soil systems to warming, particularly changes in soil–water and –energy budgets, and soil biogeochemical processes such as carbon and nitrogen cycling. Experimental methods for soil and ecosystem warming include temperature controlled environments in laboratory and greenhouse settings, moving intact soil cores across natural environmental gradients, and heating of soils in situ using various active and passive approaches (Aronson and McNulty, 2009). All of these methods have their short-comings, e.g., extrapolating results from controlled environments to the field, requirement of aboveground enclosures for passive in situ soil heating, and equipment and operational costs associated with active in situ heating. Currently, an inexpensive and effective alternative for in situ soil heating that does not require an aboveground enclosure is lacking.

Soil and ecosystem heating methods vary widely and have been reviewed in detail in Rustad et al. (2001), Shaver et al. (2000) and Aronson and McNulty (2009). Here we highlight several of the main passive and active methods used in previous field studies as context for the approach tested in this work. Many studies apply active heating methods such as infrared heaters (Harte et al., 1995), cables buried in the soil (Peterjohn et al., 1993), with more recent approaches including a combination of steam injection and passive aboveground enclosures (Hanson et al., 2011). Active methods effectively heat above- and below-ground systems with significant changes observed as a result of heating in plant species composition, soil respiration, and soil–water content (Shaver et al., 2000). However, these methods are expensive in terms of equipment set up, operational costs and energy consumption, and require proximity and access to electricity. Passive methods generally include open top chambers and greenhouses placed over mesocosm plots in the field (Kennedy, 1995); however these approaches exclude and minimize the turbulent transfer of air, energy and water vapor, and the movement of mass into and out of the experimental enclosure. Another passive heating approach consists of nighttime trapping of longwave radiation from the soil with an IR reflective sheet above the soil surface that effectively warms the soil overnight (Beier et al., 2004). However, this requires an automated system to lower the IR sheet over the soil surface in the evening and to raise the IR sheet in the morning.

Here we present a simple, inexpensive in situ passive soil heating approach based on easy to construct IR mirrors that do not require automation or enclosures. The objective of this work was to empirically test the efficacy of these mirrors for heating the soil surface and shallow subsoil under field conditions.

2 Materials and methods

2.1 Infrared mirror design

The infrared mirrors consisted of 61 × 61 cm glass panels mounted in a 5 × 5 cm redwood board frame (Fig. 1). The glass panels were mounted in the frame at a height of 15.25 cm above the ground surface; with the 5 × 5 redwood frame this leaves and air gap of 10 cm between the bottom of the frame and the ground to allow of air flow and mixing around the base of the panel. The panel glass consisted of common double strength window glass 3 mm thick. The side of the glass away from the plot was covered with Gila Titanium heat control window film (Eastman Chemical Performance Films Division, Gila Film Products, St. Louis, MO, USA). The frames in the field were mounted facing true south, tilted back 10° from vertical (top of frame tilts away from the plot), and secured with metal t-posts. The glass absorbs ultraviolet light and the film reflects up to 72 % of incoming solar radiation towards the soil surface.

2.2 Field experiments

The mirrors were tested using a series of field experiments designed to quantify the effect of mirrors on surface and shallow subsurface soil temperature. The experiments consisted of a set of initial field trials followed by a larger scale test with multiple replicated plots on different soil types. The size of the mirrors is best suited to heating soil in low-stature ecosystems, making them ideal for grassland, short scrub, tundra, and agriculture studies.

2.2.1 Initial field trials

Initial field trials were carried out at the Karsten Turfgrass Research Facility located at the University of Arizona Campus Agricultural Center (CAC) in Tucson, AZ at 32°16′51.77″ N, 110°56′13.14″ W, at an elevation of 715 m a.s.l. The average climate at this location includes a mean annual air temperature of 22.4 °C, mean annual potential evapotranspiration of 1945 mm yr^{-1}, and mean annual precipitation of 275 mm yr^{-1} characterized by a bimodal precipitation regime where ~ 50 % of precipitation derives from cool, winter rains and ~ 50 % arrives during the summer as part of the North American Monsoon, with warm dry periods in the spring and fall. Meteorological data for 2013, the year of observation, fell within climatological norms with a mean temperature of 20.4 °C, potential evapotranspiration of 1933 mm, and annual precipitation of 190 mm. Meteorological data were measured hourly at the CAC using a weather station managed as part of the Arizona Meteorological Network following standard techniques. The station is < 0.5 km from the study site and data are freely available online (AZMET; http://ag.arizona.edu/azmet/). The soil at the study area was classified as a coarse-loamy over skeletal, mixed, superactive, calcareous, hyperthermic Typic Torrifluvent (http://websoilsurvey.sc.egov.usda.gov/App/WebSoilSurvey.aspx), with a fine sandy loam surface soil that contains 4–7 % clay based on hand texturing, and < 0.5 % organic matter. The parent material was granitic alluvium from the Rillito River and associated local drainages.

The mirrors were placed in an area free of vegetation and groundcover to facilitate direct heating of the soil surface. The initial mirror array consisted of three mirrors facing south; the central mirror facing due south, with a mirror on each side at an angle of 130° relative to the south facing mirror. The side mirrors resulted in significant shading of the plot in morning and early evening. As such, following an initial monitoring period of three months starting in March 2013, the side mirrors were removed in sequence, leaving only the central south facing mirror. Data were collected for an additional three months starting in June 2013 following side mirror removal.

Surface and shallow subsurface soil temperature were recorded using 12 bit Temperature Smart Sensor (S-TMB-M006) attached to an HOBO Micro Station Data Logger (H21-002; Onset Computer Corporation, Bourne, MA, USA) set to record on a 15 min interval. The surface thermocouple was placed directly on the soil surface and the shallow subsurface probe was placed 5 cm below the soil surface. Control thermocouples were placed adjacent to the mirror plot and linked to the same data-logger; roughly 1 m separated the control and test plots.

2.2.2 Replicated plots

The replicated field experiment was also located at the CAC in a field adjacent to the test plot location and was part of a larger project examining the role of soil amendments on native vegetation establishment in topsoil removed and stockpiled from an open pit mine. The two soils used in this experiment were collected at 31°50′34.30″ N, 110°45′05.96″ W, 1615 m a.s.l., and 31°49′20.48″ N, 110°44′03.62″ W, 1500 m a.s.l., and mapped as the Chiricahua and Hathaway soil series, respectively (http://websoilsurvey.sc.egov.usda.gov/App/WebSoilSurvey.aspx). The Chiricahua soil (CHIR) was derived from a mix of metamorphic rocks and classified as an Ustic Haplargid; the Hathaway soil (HATH) was derived from mixed sedimentary rocks, largely sandstone, and classified as an Aridic Calciustoll (https://soilseries.sc.egov.usda.gov/osdname.asp). The soils were excavated mechanically to a depth 1.75 m below the soil surface and delivered to the CAC. Soils were sieved in the field to remove coarse fragments > 15 cm in diameter before placement in experimental mesocosms.

The replicated field plots consisted of mesocosms constructed at the CAC. Soils were added to a depth of 30 cm to mesocosms 0.91 m on a side after the existing surface had been removed and covered with geotextile fabric. The experimental design was a randomized complete block with each mesocosm randomly assigned to soil type, control, and mirror treatments. Plots with mirror treatments were equipped with two adjacent mirrors oriented due south, tilted back 10° from vertical, and secured with metal t-posts (Fig. 1).

The CHIR and HATH soils varied in texture and coarse fraction content, color, and organic matter. Particle size analysis was quantified by LPSA following removal of organic matter. Weight percent coarse fragments was quantified as the fraction not passing a 2 mm sieve. Dry and moist soil color were measured using a Spectron CE-590 spectroradiometer (Spectron Instruments, Denver, CO) and converted to Munsell notation, and organic matter quantified as loss on ignition (LOI) following 2 h combustion at 500 °C. Soil properties were measured at University of Arizona Center for Environmental Physics and Mineralogy. Soil color was used to estimate dry and moist soil albedo (0.3–2.8 µm) (α) following Post et al. (2000) as: $\alpha = 0.069v - 0.114$, where v is the Munsell soil value. The volumetric heat capacity of the different soils in each mesocosm, C_T, was calculated as (Jury et al., 1991; Kluitenberg, 2002): $C_\mathrm{T} = (C_\mathrm{O}X_\mathrm{O} + C_\mathrm{S}X_\mathrm{S} + C_\mathrm{R}X_\mathrm{R})(1 - \phi_\mathrm{T})$, where C_O, C_S, and C_R are the volumetric heat capacities of organic matter, soil, and rock with values of 2.5, 1.9, and 2.4 $\mathrm{kJ\,kg^{-1}\,K^{-1}}$, respectively (Eppelbaum et al., 2014; Kluitenberg, 2002), X_O, X_S, X_R are the volume fractions organic matter, soil, and rock in the mesocosm, and φ_T is the total porosity of the mesocosm calculated assuming the volume rock fraction has zero porosity and soil bulk density calculated following Rawls (1983). The values for C_T were calculated assuming a zero water content to provide a dry reference volumetric heat capacity for each soil type.

Repeated measures of surface soil temperature were recorded with a handheld IR thermometer (Cen-Tech model 60725, Cen-Tech, Camarillo, CA, USA) from a height of approximately 1 m above the soil surface on six dates between 20 August and 24 September 2013. Repeated measures of soil moisture measured were recorded using FieldScout TDR 100 Soil Moisture Meter (Spectrum Technologies Inc. Plainfield, IL, USA) with 10 cm probes on sixteen dates between 22 August and 15 October 2013.

Title Page
Abstract | Introduction
Conclusions | References
Tables | Figures
◀| |▶
◀ ▶
Back | Close
Full Screen / Esc
Printer-friendly Version
Interactive Discussion

2.3 Data manipulation and statistical analyses

The relative soil heating by the IR mirrors in the initial field trials was calculated as: $\Delta T = T_{\mathrm{IR}} - T_{\mathrm{C}}$; where ΔT is the relative increase or decrease in soil temperature, T_{IR} is temperature in the IR mirror plot, and T_{C} is temperature in the control plot, both in degrees Celsius. Statistical analyses included simple summary statistics for ΔT values, means comparison of control and IR plot temperature using a one-way *t* test, and correlation of ΔT to meteorological variables collected at the nearby AZMET station.

Summary statistics by mirror and soil treatments were determined for the replicated field plots, with means comparison of surface soil temperature and soil moisture (Θ_{v}) among soil and mirror treatments using simple one-way *t* tests. Temperature and moisture data were further summarized by date and the relative difference in surface temperature, ΔT, and soil moisture, $\Delta\Theta_{\mathrm{v}}$, calculated as the difference in the means for each treatment. Significance differences in ΔT and $\Delta\Theta_{\mathrm{v}}$ between soil types were determined averaging across all dates of observation. Furthermore, ΔT and $\Delta\Theta_{v}$ were correlated with local meteorological variables from the AZMET station.

3 Results and discussion

3.1 Initial field trials

The initial field trial with the three mirror array yielded substantial warming of the shallow subsurface soil (5 cm depth), with maximum midday warming near 17 °C relative to the unheated control plot (Fig. 2). Heating was greatest between the hours of 1100 and 1300 h when the sun was at its highest point in the sky with a mean ΔT of 1.1 °C. However, as the year progressed from early spring to summer and the sun moved further to the north, substantial cooling of the mirror plot was observed in the morning and evening hours, with a concurrent reduction in midday heating (Fig. 2). In particular, the afternoon temperature differential indicated the mirror plots were up to 5 °C cooler at a 5 cm depth than the control plot. The morning and afternoon cooling was due to shading from the side mirrors oriented at 130° relative to the central south facing mirror.

We conducted several short-term experiments with the three mirror array to try and address the morning and afternoon shading. The first experiment simply included changing the angle of the side mirrors from 130 to 160° relative to the central south facing mirror, between days 141 and 154. Opening the mirrors did reduce the amount of shading and increase the hours of warming, but yielded a mean ΔT value near $-0.2\,^{\circ}$C, with brief periods of 4–5 °C cooling in the afternoon hours (Table 1). The second experiment ran from day 154 to 164 and included removing the west panel to try and eliminate the afternoon cooling trend. This experiment did yield a reduction in both morning and afternoon cooling and returned the mean ΔT to an overall warming trend of 0.5 °C.

The final field trial experiment consisted of removing both side mirrors, leaving just the one south facing mirror. In this instance, soil temperature was measure both directly at the soil surface and at a 5 cm depth. The data indicated mean ΔT values of 0.5 ± 1.6 and $0.3 \pm 0.9\,^{\circ}$C at the surface (Fig. 3a) and 5 cm depth (Fig. 3b; Table 1). Both surface and 5 cm depth temperatures exhibited the greatest heating at midday, with maximum ΔT values near 10 and 5 °C, respectively. Periods of cooling were still evident in the morning and afternoon hours. Detailed observation of diurnal ΔT trends indicate cooling between the hours of 08:00 and 10:00 that was then overcome by heating during the midday hours. Of the ~ 2300 hourly average ΔT values, 64 and 67 % of observations were $\geq 0\,^{\circ}$C for surface and subsurface soils, respectively, such that the majority of observations indicated warming (Table 1).

Comparing the one-mirror ΔT values to meteorological variables indicated that the relative cooling in mirror plots was greatest during periods of high atmospheric moisture and following precipitation events when surface soils were moist (Fig. 4a). This was evidenced by significant negative trends in ΔT with both mean daily dewpoint (Fig. 4b) and daily minimum relative humidity (Fig. 4c). Both of these values provide a measure of atmospheric moisture content, with the mean daily dewpoint a daily average and minimum relative humidity providing a measure of atmospheric humidity at the hottest point in the day. These data clearly indicate that the warming effect of the mirror was minimized or negated with a wet atmosphere. This trend was particularly evident in the 5 cm depth ΔT values following rainfall events. Detailed diurnal analysis of 5 cm ΔT values indicated that during wet periods following rainfall events the midday heating from the mirror was not enough to overcome any cooling associated with morning and afternoon shading. These data were consistent with both atmospheric and soil moisture limiting temperature increases in the shallow subsurface. Furthermore, the increased energy transfer to the soil in the mirror plot may also have increased evaporation rates that would buffer any warming as energy was consumed via vaporization (e.g., Wåhlin et al., 2010). However, soil moisture was not monitored during the initial field trials. These data highlight that the greatest warming impact of mirrors was during periods with dry soil and atmospheric conditions, and also suggest the potential for changes in surface soil water balance that would lead to more evaporation and soil drying in the mirror treatments.

3.2 Replicated plot experiments

The replicated field plot experiments indicated significant heating of the soil surface with an average ΔT of +5.5 °C (Fig. 5; Table 2). These measurements were single time points collected during the midday time period; as such they represent near maximum temperature differentials based on the continuous data patterns collected in the initial field trial. The relative warming also varied significantly by soil type, with HATH exhibiting ΔT of +6.8 °C and CHIR exhibiting ΔT values of +4.1 °C (Table 2). The CHIR plots contained a larger fraction of rock fragments, lower estimated total plot porosity, and higher heat capacity that would also limit temperature change per unit of additional IR radiation (Jury et al., 1991) (Table 2).

The replicated field plot ΔT values exhibited a significant negative trend with increasing minimum daily relative humidity (Fig. 5), confirming the field test trials where warming from the mirrors was attenuated by atmospheric and soil moisture. The date that deviated most substantially from this overall trend was the last date collected on day 267. This measurement date was preceded by the largest series of rainfall events during the observation period that corresponded to increased soil moisture content in both the CHIR and HATH soils. The lack of differential heating at this time period despite relatively low minimum relative humidity values was thus likely controlled by soil moisture content.

Soil moisture data indicated a relative drying trend in the mirror plots, with significantly greater drying in the HATH relative to the CHIR soils (Fig. 6; Table 2). The CHIR soils exhibited high rock fragment content, coarse textured fine-earth fraction, and only 13 % total mesocosm porosity leading to both a limited water holding capacity and faster drainage relative to the HATH mesocoms (Table 2). This was confirmed by soil moisture data from the control mesocoms that indicated CHIR soils averaged 13.6 ± 5.9 % volumetric water content relative to 22.7 ± 10.4 % in the HATH soils and that for each day of observation, the CHIR soils were drier than the HATH soils by 5 to 15 % volumetric water content. The CHIR soils also exhibited a greater volumetric heat capacity in the solid phase that would limit the transfer of heat energy to soil water and vaporization. In contrast, the HATH soils exhibited fewer coarse fragments, greater clay and silt content, and greater porosity indicating greater water holding capacity in addition to a lower volumetric soil heat capacity of the solid fraction that favors warming of the soil and greater transfer of absorbed energy to soil water, favoring soil water vaporization. The drying results are similar to results of Harte et al. (1995) and Verburg et al. (1999) that found significant drying with IR lamps and soil heating cables, respectively.

4 Conclusions

The results presented here demonstrate proof-of-concept that the infrared mirrors tested here may be used to passively heat the near soil surface, providing an inexpensive, low-maintenance alternative to other passive and active soil heating technologies.

Title Page
Abstract Introduction
Conclusions References
Tables Figures
◂◂ ▸▸
◂ ▸
Back Close
Full Screen / Esc
Printer-friendly Version
Interactive Discussion

The mirrors as constructed were effective for soil heating in environments typified by open canopy and low canopy vegetation such as agriculture systems, desert grassland and scrub ecosystems, and possibly tundra. Heating from the infrared mirrors significantly impacted both soil warming and drying, similar to trends expected with a warming climate. Key conclusions include:

- The infrared mirrors yielded significant heating and drying of soil surface and shallow subsurface relative to un-warmed control treatments;
- Atmospheric and soil moisture attenuated IR mirror-induced soil warming;
- The warming and drying effects of the infrared mirrors was soil specific, with greater potential impact on soils with lower volumetric heat capacity.

It is important to note that the initial field trials indicated soil warming from the infrared mirrors was more pronounced in winter months when the sun was further to the south, and that periods of shading related to the frame and mirror orientation were apparent in morning and evening hours. The efficacy of soil heating with the infrared mirrors could be improved with detailed numerical modeling of coupled soil-atmosphere energy and water balances that take into account latitude, seasonal changes in sun position, and soil moisture and heat capacity, e.g., using a model such as HYDRUS 1D. Such modeling would facilitate optimization of mirror angle, size, and orientation to reach the desired experimental soil warming and drying response, making these infrared mirrors a powerful tool for experimental warming of open canopy and low vegetation canopy systems.

Acknowledgements. This work was funded by a grant from the Rosemont Copper Company. REG acknowledges support from NIFA ARZT-1360540-H12-199 and CR acknowledges NIFA ARZT-1367190-H21-155.

References

Aronson, E. L. and McNulty, S. G.: Appropriate experimental ecosystem warming methods by ecosystem, objective, and practicality, Agr. Forest Meteorol., 149, 1791–1799, 2009.

Beier, C., Emmett, B., Gundersen, P., Tietema, A., Penuelas, J., Estiarte, M., Gordon, C., Gorissen, A., Llorens, L., Roda, F., and Williams, D.: Novel approaches to study climate change effects on terrestrial ecosystems in the field: Drought and passive nighttime warming, Ecosystems, 7, 583–597, 2004.

Eppelbaum, L. V., Kutasov, I. M., and Pilchin, A.: Applied geothermics, in: Lecture Notes in Earth System Sciences, doi:10.1007/978-3-642-34023-9, Springer Berlin Heidelberg, 2014.

Hanson, P. J., Childs, K. W., Wullschleger, S. D., Riggs, J. S., Thomas, W. K., Todd, D. E., and Warren, J. M.: A method for experimental heating of intact soil profiles for application to climate change experiments, Global Change Biol., 17, 1083–1096, 2011.

Harte, J., Torn, M. S., Chang, F. R., Feifarek, B., Kinzig, A. P., Shaw, R., and Shen, K.: Global Warming and Soil Microclimate – Results from a Meadow-Warming Experiment, Ecol. Appl., 5, 132–150, 1995.

IPCC: Climate Change 2014: Synthesis Report. Contribution of Working Groups I, II and III to the Fifth Assessment Report of the Intergovernmental Panel on Climate Change, CoreWritingTeam, edited by: Pachauri, R. K. and Meyer, L. A., IPCC, Geneva, Switzerland, 2014.

Jury, W. A., Gardner, W. R., and Gardner, W. H.: Soil physics, J. Wiley, New York, 328 p., 5th edition, 1991.

Kennedy, A. D.: Simulated Climate-Change – Are Passive Greenhouses a Valid Microcosm for Testing the Biological Effects of Environmental Perturbations, Global Change Biology, 1, 29–42, 1995.

Kluitenberg, G. J.: Heat capacity and specific heat, in: Methods of Soil Analysis. Part 4 – Physical Methods, edited by: Dane, J. H. and Topp, G. C., 5, Soil Science Science of America, Madison, WI, 1201–1208, 2002.

Peterjohn, W. T., Melillo, J. M., Bowles, F. P., and Steudler, P. A.: Soil Warming and Trace Gas Fluxes – Experimental-Design and Preliminary Flux Results, Oecologia, 93, 18–24, 1993.

Post, D. F., Fimbres, A., Matthias, A. D., Sano, E. E., Accioly, L., Batchily, A. K., and Ferreira, L. G.: Predicting soil albedo from soil color and spectral reflectance data, Soil Sci. Soc. Am. J., 64, 1027–1034, 2000.

Rawls, W. J.: Estimating Soil Bulk-Density from Particle-Size Analysis and Organic-Matter Content, Soil Sci., 135, 123–125, 1983.

Rustad, L. E., Campbell, J. L., Marion, G. M., Norby, R. J., Mitchell, M. J., Hartley, A. E., Cornelissen, J. H. C., Gurevitch, J., and Gcte-News: A meta-analysis of the response of soil respiration, net nitrogen mineralization, and aboveground plant growth to experimental ecosystem warming, Oecologia, 126, 543–562, 2001.

Shaver, G. R., Canadell, J., Chapin, F. S., Gurevitch, J., Harte, J., Henry, G., Ineson, P., Jonasson, S., Melillo, J., Pitelka, L., and Rustad, L.: Global warming and terrestrial ecosystems: A conceptual framework for analysis, Bioscience, 50, 871–882, 2000.

Verburg, P. S. J., Van Loon, W. K. P., and Lukewille, A.: The CLIMEX soil-heating experiment: soil response after 2 years of treatment, Biol. Fertil. Soils, 28, 271–276, 1999.

Wåhlin, A. K., Johansson, A. M., Aas, E., Brostrom, G., Weber, J. E. H., and Grue, J.: Horizontal convection in water heated by infrared radiation and cooled by evaporation: scaling analysis and experimental results, Tellus A, 62, 154–169, 2010.

Table 1. Summary of ΔT statistics for the initial set of field trials measuring soil heating resulting from infrared mirrors.

Treatment	n^a (h)	Mean ΔT^b	Minimum ΔT (°C)	Maximum ΔT	Fraction time $\Delta T \geq 0\,^{\circ}\mathrm{C}$ (%)
Three mirrors – 130°	1898	1.1 ± 3.6^A	−9.2	16.9	75
Three mirrors – 160°	299	-0.2 ± 2.3^C	−8.2	2.9	59
Two mirrors	253	0.5 ± 1.4^B	−5.1	3.8	70
One mirror	2320	0.3 ± 0.9^B	−2.6	4.5	67

[a] Number of hours measured for each treatment.

[b] Means one standard deviation. Letters indicate significant differences using an unequal variance t test.

Table 2. Summary of soil properties for the two soil types included in the replicated field plot experiment.

Soil type	Texture class	LOI[a]	Org. C[a]	Rock[a] (wt. %)	Sand	Silt	Clay	Munsell Color		Soil Albedo		φ_T (%)	C_T ($MJ\,m^{-3}\,K^{-1}$)	Mean ΔT[b] (°C)	Mean $\Delta\theta_v$[b] (%)
								Dry	Moist	Dry	Moist				
Chiricahua – CHIR	sandy loam	3.5 ± 0.01	0.7 ± 0.01	72 ± 3.2	69.1	24.4	6.4	6.90YR 3.61/2.64	5.52YR 2.75/2.6	0.135	0.076	13.2	2.02	4.1 ± 1.4^B	-1.0 ± 2.0^B
Hathaway – HATH	sandy loam	4.3 ± 0.05	1.0 ± 0.02	43 ± 3.6	59.7	30.9	9.4	7.7YR 3.88/1.82	7.29YR 2.61/1.74	0.154	0.066	31.4	1.50	6.8 ± 2.0^A	-6.0 ± 3.8^A

[a] Loss on ignition (LOI), organic carbon, and rock fragments. Values are mean of three replicates reporting one standard deviation

[b] Means and one standard deviation. Letters indicate significant differences using an unequal variance *t* test.

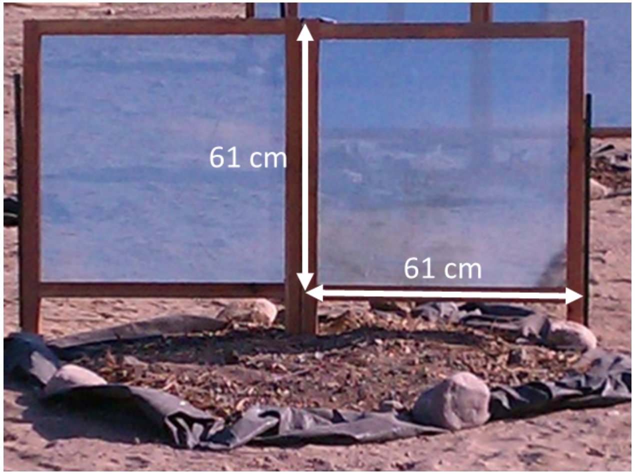

Figure 1. Example of the infrared mirror design showing the two 61 × 61 cm panel design that was implemented for the replicated plot field trial. This photo was taken mid-morning with the sun to the east; note the shading induced by the mirror frame in the experimental plot.

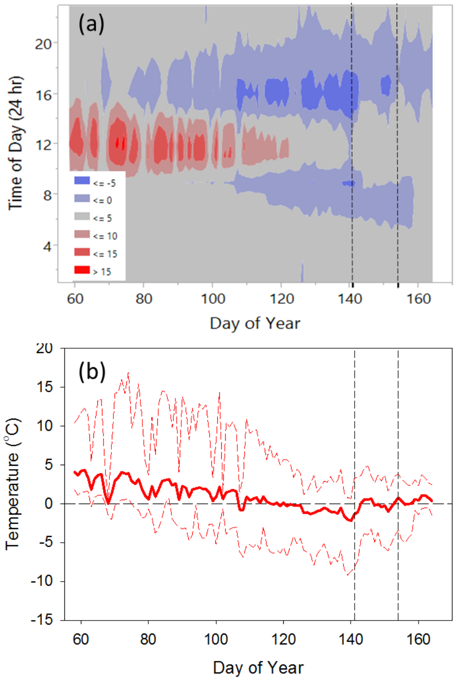

Figure 2. Contour plot of relative soil heating, Δ*T* (°C), by day of year and time of day **(a)** and daily mean (bold red line) and minimum and maximum (dashed lines) Δ*T* by day of year **(b)**. The vertical dashed lines in **(a)** and **(b)** represent changes from the three mirror array, to the two mirror array, and finally the one mirror array.

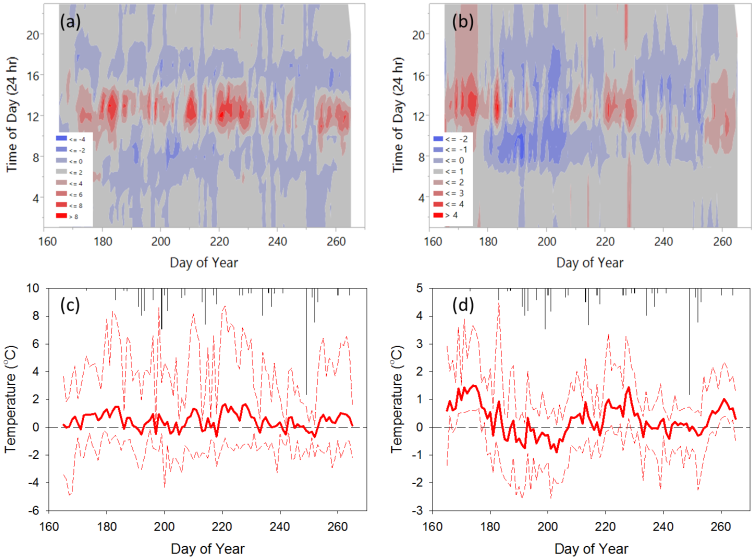

Figure 3. Contour plot of relative soil heating, ΔT (°C), by day of year and time of day for soil surface **(a)** and shallow subsurface (5 cm depth) **(b)** for the one infrared mirror array. Daily mean (bold) and minimum and maximum (dashed lines) ΔT values for the surface **(c)** and shallow subsurface **(d)**. Black bars on the upper x axis are daily precipitation totals from the nearby meteorological station.

Title Page
Abstract
Introduction
Conclusions
References
Tables
Figures
◄
►
Back
Close
Full Screen / Esc
Printer-friendly Version
Interactive Discussion

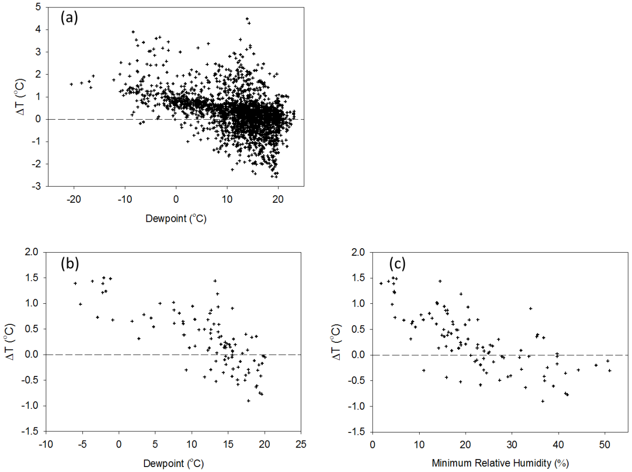

Figure 4. Relative soil heating, ΔT (°C), compared to dewpoint (°C) for all hourly measurements from the one panel array **(a)**. Daily average ΔT relative to daily average dewpoint **(b)** and daily minimum relative humidity (%) **(c)**. The dashed line on the y axis indicates a ΔT value of zero with values greater than zero indicating heating and values less than zero indicating cooling as a result of the infrared mirror treatment.

Title Page
Abstract | Introduction
Conclusions | References
Tables | Figures
I◄ | ►I
◄ | ►
Back | Close
Full Screen / Esc
Printer-friendly Version
Interactive Discussion

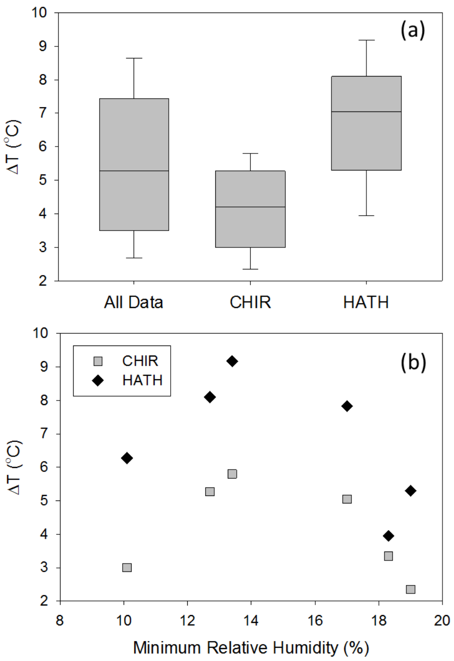

Figure 5. Box plots of relative soil heating, ΔT (°C), for all data from the replicated field experiment (all data) and for data separated by soil type (Chiricahua, CHIR; and Hathaway, HATH) **(a)**, and mean daily relative soil heating ΔT compared to daily minimum relative humidity for the two soil types **(b)**.

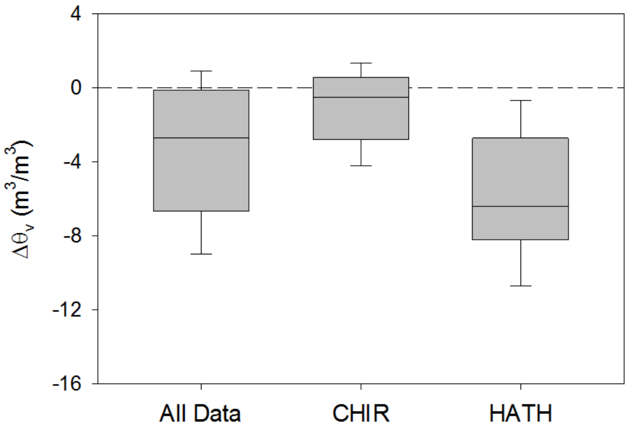

Figure 6. Box plots of relative change in volumetric soil water content, $\Delta\Theta_v$ ($m^3\,m^{-3}$), for all data from the replicated field experiment (All Data) and for data separated by soil type (Chiricahua, CHIR; and Hathaway, HATH).